Asian Journal of Pharmaceutical Sciences 14 (2019) 423–434

Available online at www.sciencedirect.com

ScienceDirect

journal homepage: www.elsevier.com/locate/AJPS

Original Research Paper

A hybrid genipin-crosslinked dual-sensitive hydrogel/nanostructured lipid carrier ocular drug delivery platform

Yibin Yu[a], *Ruoxi Feng*[a], *Jinyu Li*[a], *Yuanyuan Wang*[a], *Yiming Song*[a], *Guoxin Tan*[a], *Dandan Liu*[b], *Wei Liu*[c], *Xinggang Yang*[a], *Hao Pan*[d,*], *Sanming Li*[a,**]

[a] *Shenyang Pharmaceutical University, Shenyang 110016, China*
[b] *Liaoning Institute of Science and Technology, Benxi 117004, China*
[c] *Zhengzhou University, Zhengzhou 450001, China*
[d] *Liaoning University, Shenyang 110016, China*

ARTICLE INFO

Article history:
Received 29 May 2018
Revised 9 August 2018
Accepted 22 August 2018
Available online 10 September 2018

Keywords:
Ocular drug delivery
Nanostructured lipid carrier
Semi-IPN hydrogel

ABSTRACT

The objective of this study was to develop a novel hybrid genipin-crosslinked dual-sensitive hydrogel/nanostructured lipid carrier (NLC) drug delivery platform. An ophthalmic anti-inflammatory drug, baicalin (BN) was chosen as the model drug. BN–NLC was prepared using melt-emulsification combined with ultra-sonication technique. Additionally, a dual pH- and thermo-sensitive hydrogel composed of carboxymethyl chitosan (CMCS) and poloxamer 407 (F127) was fabricated by a cross-linking reaction with a nontoxic crosslinker genipin (GP). GP-CMCS/F127 hydrogel was characterized by FTIR, NMR, XRD and SEM. The swelling studies showed GP-CMCS/F127 hydrogel was both pH- and thermo-sensitive. The results of *in vitro* release suggested BN–NLC gel can prolong the release of baicalin comparing with BN eye drops and BN–NLC. *Ex vivo* cornea permeation study was evaluated using Franz diffusion cells. The apparent permeability coefficient (P_{app}) of BN–NLC gel was much higher (4.46-fold) than that of BN eye drops. Through the determination of corneal hydration levels, BN–NLC gel was confirmed that had no significant irritation to cornea. *Ex vivo* precorneal retention experiments were carried out by a flow-through approach. The results indicated that the NLC-based hydrogel can prolong precorneal residence time. In conclusion, the hybrid NLC-based hydrogel has a promising potential for application in ocular drug delivery.

* Corresponding author. Liaoning University, No.66, Chongshan Middle Road, Shenyang 110016, China.
** Corresponding author. Shenyang Pharmaceutical University, No.103, Wenhua Road, Shenyang 110016, China.
E-mail addresses: haopan0330@163.com (H. Pan), li_sanming@126.com (S. Li).
Peer review under responsibility of Shenyang Pharmaceutical University.

https://doi.org/10.1016/j.ajps.2018.08.002

1. Introduction

Eye is a distinctive organ because of unique drug disposition features. For treating various eye disorders, topical administration to the eye is the most accessible and common route due to its convenient and painless properties. Nonetheless, the drug bioavailability of conventional eye drops is relatively low as a result of inherent defense mechanisms of the eye, including low permeability of the cornea, constant lachrymation, frequent blinking and rapid nasolacrimal drainage [1–3]. An ideal ophthalmic drug delivery system can not only facilitate drug to penetrate through the corneal barriers, but also prolong the pre-corneal retention time.

Hydrogels are hydrophilic polymers which are insoluble but can absorb a large amount of water in aqueous media [4–6]. Since the pioneering work of Wichterle et al. in the early 1960s on the synthetic hydrogel, the applications of hydrogels have been broadened to many fields, such as food additives, regenerative medicine, tissue engineering and drug delivery [5,7–11]. In particular, "smart" hydrogels which can respond to outside environmental stimuli, like pH, temperature, and ionic strength, have been intensively studied [12–19]. Interpenetrating polymer networks (IPN) compose of a blend of polymers in network form where at least one component is polymerized and/or crosslinked [5,20]. Hydrogels formed by IPN mostly possess more attractive mechanical properties, attributed to not only individual crosslinked networks but physical entanglements among the polymers [13]. Moreover, hydrogels with unique properties can be fabricated by IPN. For instance, the combinations of pH- and thermo-sensitive polymers have been employed to form the "smart" hydrogel with dual pH- and thermo-sensitivity [21,22]. Semi-IPN, one type of IPN, are the interpenetrating polymer networks in which only one component of the IPN is crosslinked or polymerized [5,20].

Individual polymer based hydrogel with environment-sensitivity for ocular drug delivery, such as poloxamer hydrogels and carbomer hydrogels, have been extensively studied [23–26]. However, they have shortcomings more or less. One limitation of poloxamer hydrogels for ocular drug delivery is that the concentration of poloxamer in thermo-sensitive hydrogel is usually higher than 20% (w/w) to exhibit suitable thermoreversible properties, which has potential irritation to eyes [23,24]. Additionally, the drawbacks of poloxamer hydrogels, including low mechanical strength, poor mucoadhesion and easy dissolution in tear fluid, also limit their applications in the field of ophthalmic drug delivery [24,27–29]. To carbomer hydrogels, the pH-sensitivity comes from numerous carboxyl groups of carbomer. The acid nature of carbomer could not be neutralized by the tear fluid and hence would irritate the ocular tissue, when the polymer used in high concentration [24]. Therefore, we have fabricated a dual pH- and thermo-sensitive hydrogel composed of carboxymethyl chitosan (CMCS, pH-sensitive polymer) and poloxamer 407 (F127, thermo-sensitive polymer) by a covalent crosslinking with a nontoxic crosslinker genipin (GP). The combination of two environment-sensitive polymers can drop off the required concentration of individual polymer, improve the mechanical strength of the hydrogel and strengthen the response in terms of making the developed hydrogel responsive to multiple stimuli. Accordingly, the developed hydrogel can prolong the precorneal residence time of the drug and lower the irritation to the eye. GP can form covalent bonds with primary amine groups, which is able to crosslink macromolecules, such as chitosan, carboxymethyl chitosan and gelatin [14,30–33]. Furthermore, compared with other chemical crosslinkers, naturally occurring GP is a promising selection for crosslinking in terms of admirable biocompatibility and low cytotoxicity, which has been demonstrated to be about 10 000 times less cytotoxic than glutaraldehyde [32,34]. As previously reported, GP has been employed to fabricate hydrogels for ocular drug delivery [32,35–37]. In addition, GP is the major active anti-inflammatory ingredient in gardenia fruit, which has been used as an anti-inflammatory drug in traditional Chinese medicine for thousands of years [36,38–40].

Nanostructured lipid carriers (NLC), which can promote corneal penetration, control drug release, avoid organic solvents during production, have been regarded as promising tools for ocular drug delivery recently [1,2,41]. NLC also have the ability to immobilize drugs and prevent the nanoparticles from coalescing because of the solid matrix. However, NLC may still be rapidly eliminated by defense mechanisms of the ocular globe, owing to their low viscosity. To circumvent this drawback, NLC can be gelled or incorporated into semi-solid systems to increase the viscosity of the drug delivery system and consequently increase the retention time on ocular surface [42,43].

In present study, we fabricated a novel NLC-based hydrogel for ocular delivery of baicalin (BN), an ophthalmic anti-inflammatory drug [44,45]. BN–NLC was prepared, characterized and incorporated into the hydrogel. GP-CMCS/F127 hydrogel was synthesized under a simple, facile and green fabrication process without complicated procedure, high temperature or usage of organic solvent. IR, NMR, XRD and SEM were performed to demonstrate the successful formation of GP-CMCS/F127 hydrogel. In addition, swelling properties of GP-CMCS/F127 hydrogel were investigated under different pH and temperature. Moreover, the superiorities of BN–NLC gel over BN eye drops and BN–NLC for ophthalmic delivery were evaluated concerning *in vitro* release, *ex vivo* cornea permeation and *ex vivo* precorneal retention studies.

2. Materials and methods

2.1. Materials

Baicalin (BN) was obtained from Shanxi Zelang Phytoextraction Co., Ltd. (Xi'an, China). Compritol 888 ATO, a hydrophobic mixture of mono-, di- and tri-behenate of glycerol, was kindly gifted by Gattefosse (Paris, France); Miglyol 812N, mixtures of Caprylic/Capric Triglycerides, was provided by Sasol (Witten, Germany); Soy lecithin was supplied by Taiwei pharmaceutical Co., Ltd. (Shanghai, China); Cremophor EL was provided by BASF (Ludwigshafen, Germany). Carboxymethyl chitosan (CMCS, Mw = 197.17 kDa) was supplied by Eisie Chemical Co., Ltd (Zhejiang, China); Poloxamer 407 (F127) was acquired from BASF (Ludwigshafen, Germany); Genipin (GP) was provided by Challenge Bioproducts (Taichung, Taiwan). Coumarin-6 (C6)

Table 1 – Feed compositions for the formation of GP-CMCS/F127 hydrogels.

Sample	CMCS (%, w/v)	F127 (%, w/v)	GP (%, w/v)	Water (ml)
1	3.0	1.0	0.2	10
2	3.0	1.0	0.4	10
3	3.0	1.0	0.8	10
4	2.5	1.5	0.4	10
5	3.5	0.5	0.4	10

was supplied by Aladdin Co., Ltd (Shanghai, China). All other reagents were of analytical grade or better.

2.2. Animals

Ocular damage free, New Zealand albino rabbits (half male and half female, weighting 1.5–2.0 kg), were supplied by the Lab Animal Center of Shenyang Pharmaceutical University. The rabbits, fed with standard pellet diet and water *ad libitum*, housed in standard cages in a light-controlled room at 25 ± 1 °C and 50% ± 5% R.H. Animal studies were approved by Shenyang Pharmaceutical University Animal Ethical Committee and performed according to the Principles of Laboratory Animal Care (NIH publication No. 92-93, revised in 1985).

2.3. Preparation of different formulations

2.3.1. Preparation of BN–NLC

BN loaded NLC was prepared using the melt-emulsification and ultra-sonication method [46]. Compritol 888 ATO (110 mg), Miglyol 812N (90 mg) and baicalin (8 mg) were mixed and heated under magnetic stirring at 87 °C to form a uniform lipid phase. Simultaneously, the aqueous surfactant solution with Cremophor EL (150 mg) and soy lecithin (150 mg) was prepared in 10 ml deionized water and also heated at 87 °C. The hot surfactant solution was then dropped to the hot lipid under magnetic stirring for 5 min. A probe-ultrasonic cell disruptor was employed to homogenize the coarse emulsion for 2 min and the obtained dispersion was quickly placed in an ice bath to promote the formation of the nanostructured lipid carriers.

2.3.2. Preparation of BN–NLC gel

The hydrogel composed of carboxymethyl chitosan (CMCS) and poloxamer 407 (F127) crosslinked by genipin (GP) was developed to obtain a dual pH- and thermo-sensitive semi-IPN hydrogel (Fig. 1). Different hydrogels were fabricated by choosing different weight ratios of CMCS to F127 and different concentrations of GP (Table 1). CMCS and F127 were both dissolved in 5 ml deionized water and they were mixed. Subsequently, we added GP slowly to the mixed solution under shaking at 37 °C and the crosslinking reaction lasted for 2 h. Then the hydrogel was held for 24 h at room temperature, dialyzed by a cellulose membrane (8 000–14 000 Mw t.) for 24 h and afterwards lyophilized. The swelling-loading method was chosen to incorporate BN–NLC into the hydrogel [47]. In brief, the lyophilized hydrogel was immersed in BN–NLC dispersion at room temperature for 24 h. Then the swollen hydrogel was carefully taken out from BN–NLC dispersion, and we wiped off water excess on the surface of the swollen hydrogel with filter paper.

2.3.3. Preparation of BN eye drops

10 ml of 15% propylene glycol was employed to dissolve 2 mg baicalin to obtain BN eye drops, which was used as the negative control in present study [48].

2.4. Physicochemical characterization

2.4.1. Characterization of particles

The particle size (PS) and polydispersity index (PDI) were analyzed with a ZetasizerNano ZS90 (Malvern Instruments, UK). TEM studies were carried out by negative-staining method, using a JEM-2100 JEOL instrument (Tokyo, Japan).

2.4.2. Determination of entrapment efficiency

The entrapment efficiency (EE, %) of BN–NLC was determined by centrifugal ultrafiltration method [2]. Briefly, 400 µl NLC sample was added into the ultrafiltration tube and centrifuged for 30 min at 4000 rpm. Unentrapped baicalin was acquired in the ultrafiltrate, which was analyzed by HPLC at 280 nm. The HPLC system with a Diamonsil C_{18} column (250 mm × 4.6 mm, 5 µm, Dikma, China) was employed to measure the concentration of baicalin. Additionally, 400 µl NLC sample was directly precipitated with methanol and metered to 2 ml. After centrifugation of 30 min at 4000 rpm, the total baicalin in BN–NLC was acquired in the supernatant and quantified by HPLC after filtering through 0.22 µm membrane filters. EE was calculated from the following equation:

$$EE\% = \frac{C_{Total} - C_{Free}}{C_{Total}} \times 100$$

where C_{Total} is the concentration of total baicalin and C_{Free} is the concentration of unentrapped baicalin in the ultrafiltrate.

2.4.3. Stability of BN–NLC dispersed into the hydrogel

Dynamic light scattering (DLS) was employed to evaluate the stability of BN-NLC incorporated into the hydrogel for seven consecutive days. Freshly prepared samples were stored at 4 °C. Every 24 h, particle size (PS) and polydispersity index (PDI) of samples were determined.

2.5. Characterization of GP-CMCS/F127 hydrogel

2.5.1. IR

FTIR spectra were recorded using KBr disks on an IFS55 spectrometer (Bruker, Germany) at room temperature at wavelength range of 4000–500 cm^{-1}.

2.5.2. ^1H NMR

^1H NMR studies were carried out by a Bruker AVANCE 600 spectrometer (Bruker, Germany) using D_2O or DMSO-d_6 as the solvent.

2.5.3. XRD

X-ray diffraction patterns were obtained by a D8 X-ray diffractometer (Bruker, Germany), using Cu K radiation ($\lambda = 0.154$ nm). The angular range (2θ) covered was between 10° and 40°, with a scanning speed of 2°/min.

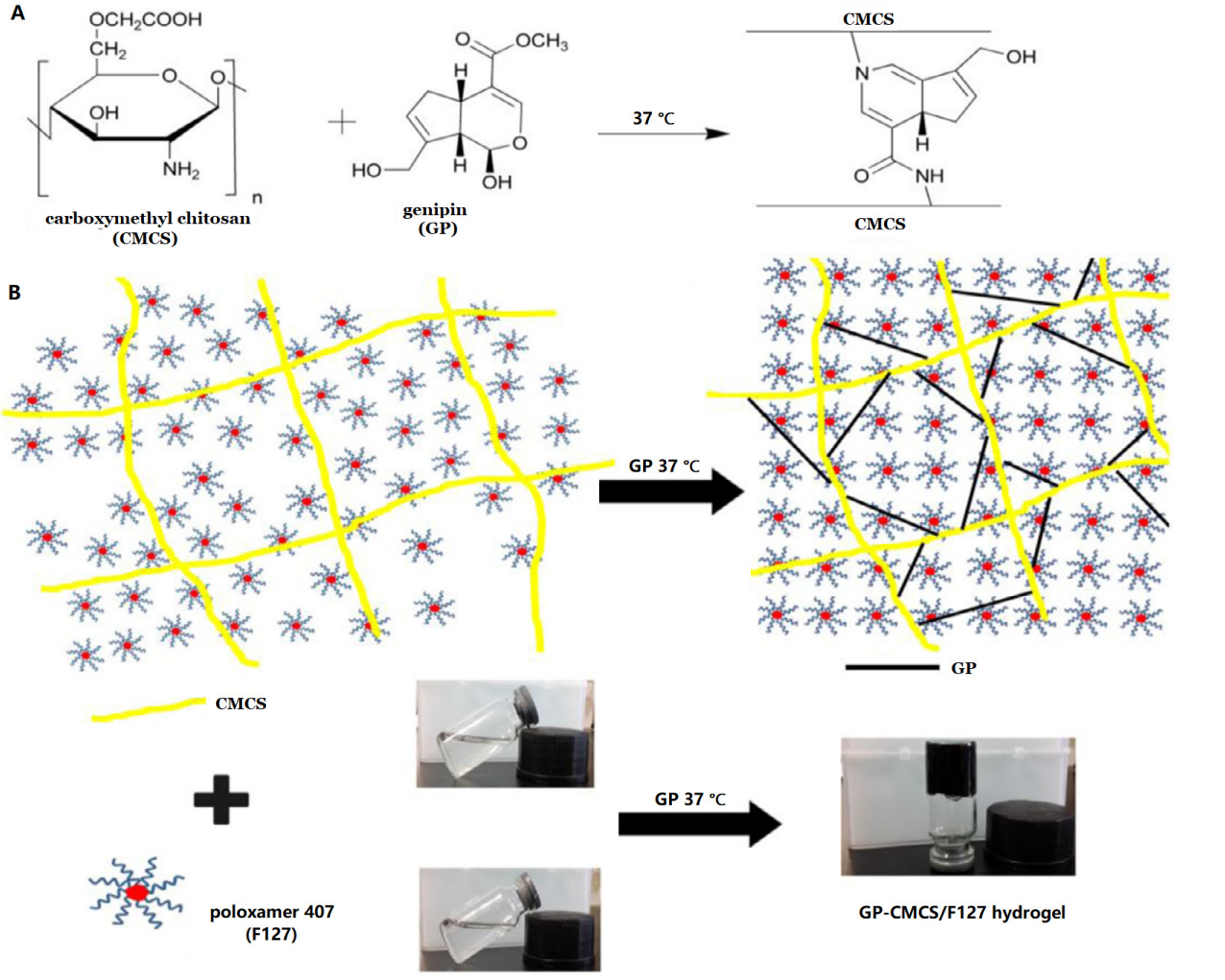

Fig. 1 – (A) Crosslinking reaction between CMCS and GP. (B) Schematic diagram of the semi-IPN formation of GP-CMCS/F127 hydrogel.

2.5.4. *Viscosity*

Viscosity measurements of F127, CMCS and GP-CMCS/F127 hydrogel were performed by a SNB-1 viscometer (Fangrui, China) at 1 rpm using the spindle of 29 at 35 °C.

2.5.5. *SEM*

Hitachi S-3400N scanning electron microscope (SEM) was employed to investigate the morphology of F127, CMCS and GP-CMCS/F127 hydrogel.

2.6. *Swelling properties*

The lyophilized GP-CMCS/F127 hydrogels were weighed (W_0) before being immersed in PBS (phosphate buffer saline, pH 6.5 or 2.5) at different temperatures (35 or 25 °C). Periodically, the immersed hydrogels were taken out from PBS. We used filter paper to wipe off water excess on the surface of the swollen hydrogel, and weighed (W_s). Swelling ratio (SR%) of GP-CMCS/F127 hydrogel was calculated from the following formula:

$$SR\% = \frac{W_s - W_0}{W_0} \times 100$$

where W_s is the weight of wet hydrogel and W_0 is the weight of lyophilized hydrogel.

2.7. *In vitro release study*

In vitro release experiments were performed by dynamic dialysis method [45]. Dialysis bags (molecular weight cut off 8 000–14 000) were used to contain various formulations of baicalin and fixed on the stirring paddles. The experiments were carried out at 35 ± 0.5 °C in 100 ml of the release medium (PBS, pH 6.5) with a constant speed (100 rpm). Periodically, 1 ml aliquots of the buffer medium containing baicalin were withdrawn and replaced with 1 ml preheated fresh release medium. The baicalin content released was analyzed by HPLC at 280 nm.

2.8. Corneal permeation study

Corneal permeation profiles of various BN formulations were studied in Franz-type diffusion cells (Tian Mei Da Instruments, Shenyang, China). Freshly excised corneas (approximate available areas 0.50 cm^2) with a nearly 2 mm sclera ring were mounted on the diffusion cells, kept at a stirring speed of 50 rpm at 34 ± 0.5 °C. 1 ml of preparations and 4 ml of PBS (pH 6.5) were placed in the donor and receptor chamber, separately. Periodically, 1 ml aliquots of diffusion medium containing baicalin were withdrawn and replaced with 1 ml preheated fresh diffusion medium. The baicalin content in the samples was analyzed by HPLC at 280 nm. The cumulative penetration amount of baicalin at different intervals was obtained by the following equation:

$$Q_n = \frac{V_0}{A}\left(C_n + \frac{V}{V_0}\sum_{i=1}^{n-1} C_i\right)$$

where V_0 is the volume of PBS in the receptor chamber (4.0 ml); A is the diffusion area (0.50 cm^2); V is the sampling volume (0.4 ml); C_n is the baicalin concentration in the receptor chamber at different intervals; and C_i is the baicalin concentration in the receptor chamber before determination. The rate of baicalin penetration was determined by the apparent permeability coefficient (P_{app}) and steady-state flux (J_{ss}) by the following equation:

$$P_{app} = \frac{\Delta Q}{\Delta t \cdot C_0 \cdot 60}$$

$$J_{ss} = C_0 P_{app}$$

where $\Delta Q/\Delta t$ is the steady-state slope of linear plot of the amount of baicalin in the receiving chamber *vs.* time, C_0 is the initial concentration of baicalin in the donor chamber.

2.9. Corneal hydration level study

The wet corneal weights were determined for the treated corneas, which were carefully removed from the scleral ring after corneal penetration tests [49]. Subsequently, the corneas were dried at 100 °C for 6 h and weighed again. The hydration level (HL%) of the cornea sample was obtained from the following formula:

$$HL\% = \left[1 - \left(\frac{W_d}{W_w}\right)\right] \times 100$$

where W_d is the dry cornea weight and W_w is the corresponding wet cornea weight.

2.10. Precorneal retention study

Ex vivo precorneal retention experiments were carried out as previously reported in Irmukhametova et al. [50]. The viscosity and moisture retention ability of different coumarin-6 (C6) formulations on cornea were studied using a fluorescence microscope (Olympus BX50, Tokyo, Japan). Freshly excised corneas were obtained after the rabbits were slaughtered. The background microscopy images were taken for each cornea and then 40 µl of C6 formulations was added onto the surface of the cornea. For each wash, 20 ml of simulated tear fluid (STF) was dripped onto the surface of the cornea at 3 ml/min with a syringe pump [50]. STF was obtained by dissolving 0.061 g $CaCl_2$, 2 g $NaHCO_3$ and 6.7 g NaCl in 1000 ml deionized water. The microscopy images were taken again after each wash, under the emitted green light. The images were analyzed by Image J in 8-bit grayscale. The mean fluorescence values were normalized by subtracting the corresponding background fluorescence prior to administration of C6 formulations. In addition, the tests were also performed directly on glass slides without excised cornea.

Table 2 – Physicochemical characterization of BN–NLC (mean ± SD, $n = 3$).

Sample	Particle size (d-nm)	Polydispersity index	EE (%)
BN–NLC	99.64 ± 2.14	0.24 ± 0.02	89.05 ± 0.44

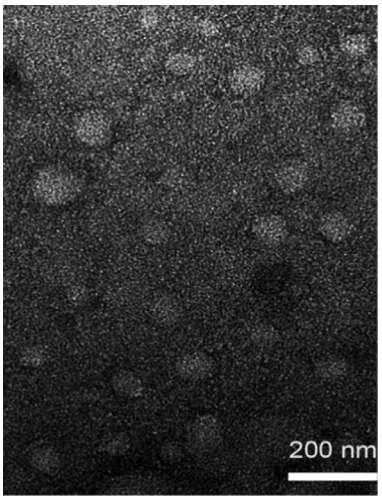

Fig. 2 – TEM micrograph of BN–NLC.

3. Results and discussion

3.1. Characterization of BN–NLC

PS, PDI and EE% of BN–NLC are presented in Table 2. To an ophthalmic drug delivery system, the particle size is important to assess the risk of irritation and discomfort to the ocular tissue. BN–NLC exhibited a relatively low size (99.64 ± 2.14 nm), which was proper for ophthalmic application. PDI value was lower than 0.3, suggesting good homogeneity. In addition, the entrapment efficiency of BN–NLC was 89.05% ± 0.44%, ascribed to liquid lipid that can disturb ordered crystalline state, form an imperfect structure in the core solid matrix, and further increase drug storage space [51]. The particle morphology of BN–NLC was characterized by TEM. As presented in Fig. 2, BN–NLC were homogeneously distributed and spherical in shape. Moreover, TEM micrograph indicated that most nanoparticles were around 100 nm, similar to the size ana-

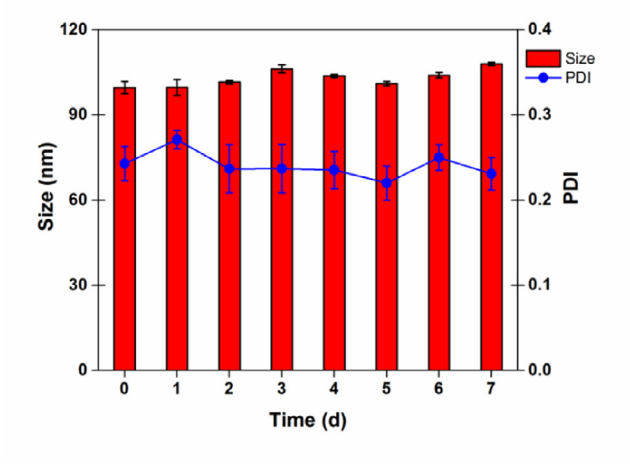

Fig. 3 – Particle size and polydispersity index of BN–NLC dispersed into the hydrogel measured for 7 d of storage at 4 °C (mean ± SD, $n = 3$).

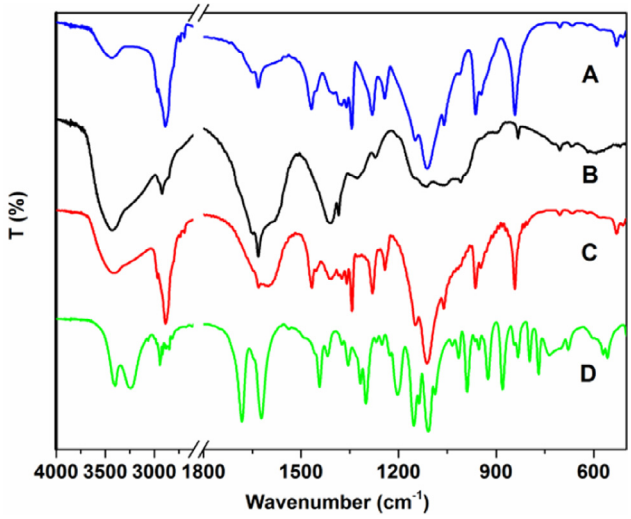

Fig. 4 – FT-IR spectra of (A) F127, (B) CMCS, (C) GP-CMCS/F127 hydrogel and (D) GP.

lyzed by dynamic light scattering (DLS). The particle size and polydispersity index of BN–NLC dispersed into the hydrogel were measured for 7 d. As exhibited in Fig. 3, the incorporation into the hydrogel did not result in particle aggregation or poor homogeneity. The results indicated that after incorporation into the hydrogel, BN–NLC kept stable within a week.

3.2. *Formation and characterization of GP-CMCS/F127 hydrogel*

GP-CMCS/F127 hydrogel was fabricated with a crosslinking reaction between CMCS and GP. The proposed mechanism of the reaction is that each GP molecule could react with two primary amine groups from two chains of different polysaccharides (Fig. 1A) [35,52]. In order to obtain a dual pH- and thermosensitive hydrogel, CMCS and F127 were blended with GP under 37 °C. The schematic illustration of the semi-IPN hydrogel is represented in Fig. 1B.

Fourier transform infrared (FTIR) spectra of GP, F127, CMCS and GP-CMCS/F127 hydrogel are exhibited in Fig. 4. GP exhibited its characteristic peaks at 1680 and 1622 cm^{-1}, owing to the stretching vibration of C = O in carboxymethyl group and C = C in cycloolefin, respectively [34,35,53]. The peaks between 3400 and 3200 cm^{-1} could be attributed to the stretching vibration of O–H [53]. The peaks of F127 were observed at 2891, 1467, 1343 and 1113 cm^{-1}, owing to the existence of –CH stretching, $–CH_2–$ bending, in-plane –OH bending and C–O stretching [47]. Broad band around 3600–3200 cm^{-1} in the CMCS spectrum could be recognized as the stretching vibration of O–H and N–H bonds [54]. The peak at 1630 cm^{-1} could be assigned to the asymmetrical stretching vibration of the COO^- group and overlapped with the deforming vibration of $-NH_2$ [14]. The absorption peak at 1409 cm^{-1} could be characteristics of the symmetrical stretching vibration of the COO^- group. The pyranose ring was evidenced by the presence of bands between 1200 cm^{-1} to 1000 cm^{-1} in the "fingerprint" region [55]. Compared to the peaks of CMCS, the peaks in the spectrum of GP-CMCS/F127 hydrogel appeared similar in whole,

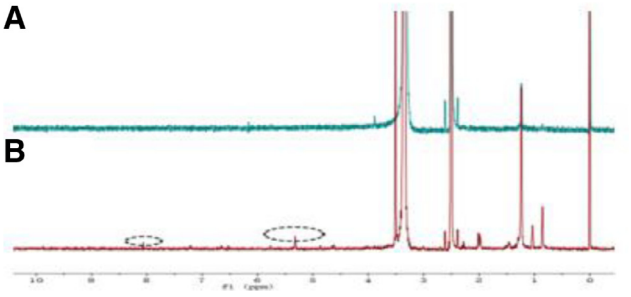

Fig. 5 – ^1H NMR comparison of (A) CMCS and (B) GP-CMCS/F127 hydrogel.

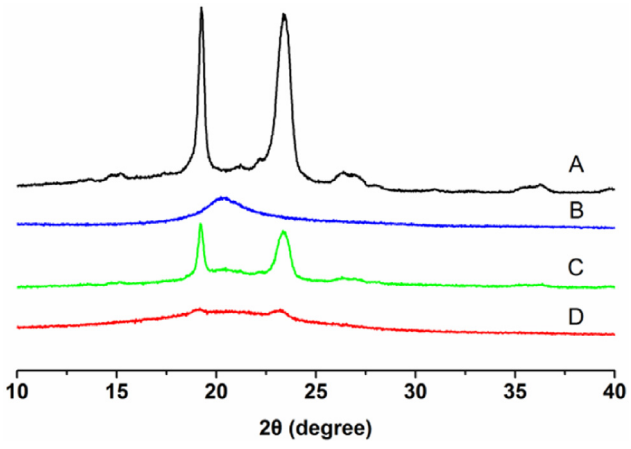

Fig. 6 – XRD patterns of (A) F127, (B) CMCS, (C) physical mixture and (D) GP-CMCS/F127 hydrogel.

but they were indeed different in detail. In the spectrum of GP-CMCS/F127 hydrogel, much smaller bands around 3600–3200 cm^{-1} and 1630 cm^{-1} were observed corresponding to the dramatic decrease of the amino groups in CMCS, and the absence at 1680 cm^{-1} was due to the drastic reduction of the carboxymethyl groups in GP [34,35,53]. The results confirmed that

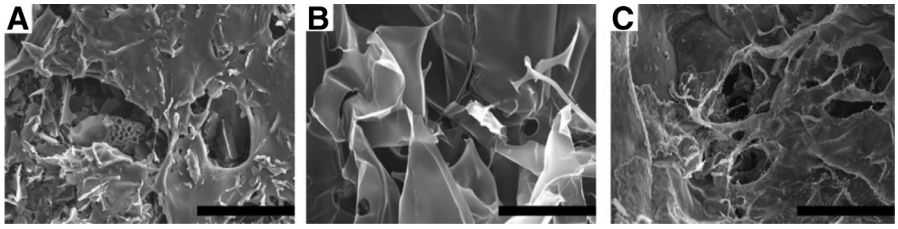

Fig. 7 – SEM micrographs of (A) F127, (B) CMCS and (C) GP-CMCS/F127 hydrogel. Scale bar is 200 μm.

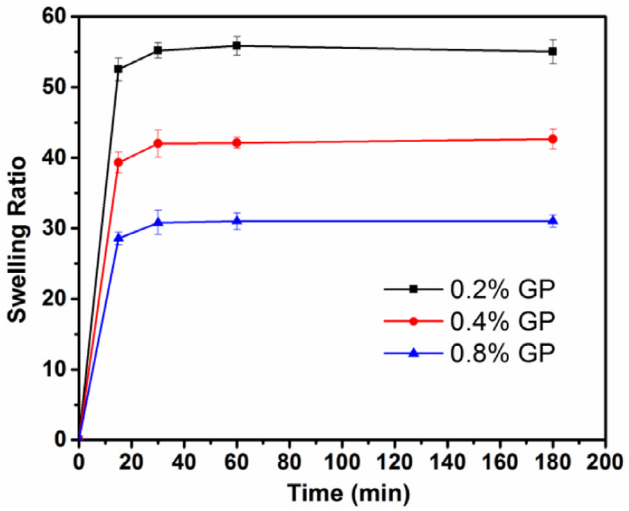

Fig. 8 – Swelling behaviors of GP-CMCS/F127 hydrogels (with the same CMCS-to-F127 weight ratio) cross-linked by various concentrations of GP (0.2%, 0.4%, 0.8%, w/v) at pH 6.5 and 35 °C (mean ± SD, $n = 3$).

the crosslinking reaction between amino groups of CMCS and carboxymethyl groups of GP had took place.

The successful cross-linking was also demonstrated by the ^{1}H NMR spectra (Fig. 5). Compared to the spectrum of pure CMCS, the appearance of new proton peaks at 8.07 ppm and 5.32 ppm in the spectrum of the synthetic hydrogel were ascribed to the protons of monosubstituted amide linked to the saccharide backbone and the alkenyl hydrogen of genipin, separately.

XRD experiments were carried out to study the crystalline information of F127, CMCS and GP-CMCS/F127 hydrogel. As presented in Fig. 6, for F127, two sharp and strong diffraction peaks positioned at $2\theta = 19.05°$ and $2\theta = 23.37°$, indicating high crystallinity nature. A broad weak peak at $2\theta = 20.23°$ could be seen in the pattern of CMCS, related to its amorphous structure. The peaks of the XRD pattern of physical mixture of F127 and CMCS hardly changed position, although the intensity was lower. Nonetheless, there was no peak in the pattern of GP-CMCS/F127 hydrogel. The formation of crystalline regions could be limited and hindered, because the crosslinking inhibits close packing of polymer chains by reducing the degree of freedom in the three-dimensional conformation [56]. XRD results further demonstrated that the crosslinking reaction occurred and the hydrogel had been synthesized.

Table 3 – Viscosity of F127, CMCS and GP-CMCS/F127 hydrogel (mean ± SD, $n = 3$).

Sample	Viscosity (Pa s)
F127	0.06 ± 0.00
CMCS	0.15 ± 0.01
GP-CMCS/F127 hydrogel	95.37 ± 1.41

Viscosity is a vital parameter to hydrogels for ophthalmic drug delivery. Adequate viscosity of the ocular formulations facilitates sustained release of the drugs and increased residence time on ocular surface, consequently ocular bioavailability [2,3,23]. The viscosity of F127, CMCS and the synthetic hydrogel was determined at the temperature of ocular surface (35 °C). As shown in Table 3, the viscosity of GP-CMCS/F127 hydrogel is much higher compared to two polymers, suggesting that the developed hydrogel has potential for application in ocular drug delivery.

The structural and morphological analyses of F127, CMCS and freeze-dried GP-CMCS/F127 hydrogel were performed by scanning electron microscopy (SEM). It is observed from Fig. 7C that GP-CMCS/F127 hydrogel had a three-dimensional network porous structure, while there was no inerratic pore on the surface of F127 and CMCS. The porous structure is beneficial to facilitate water into GP-CMCS/F127 hydrogel.

3.3. *Swelling properties*

In present study, we employed swelling ratio (SR), the index of water uptake capacity of hydrogels, to assess the swelling properties of GP-CMCS/F127 hydrogel. Time-dependent swelling behaviours of the hydrogels with the same CMCS/F127 weight ratio cross-linked by distinct concentrations of GP at pH 6.5, 35 °C, are illustrated in Fig. 8. It was obvious that the concentration of GP had a negative effect on SR of GP-CMCS/F127 hydrogel. Because higher concentrations of GP would enhance the crosslinking density, restrict the mobility of the macromolecular chains and reduce the water uptake capacity of the hydrogel. High swelling ratio is good for drug loading. And to ensure enough strength, the hydrogel cross-linked by 0.4% GP was chosen for subsequent study.

Fig. 9 exhibits the swelling properties of the hydrogels with distinct CMCS/F127 weight ratios under different pH (2.5 and 6.5) and temperature (25 and 35 °C). We could observe that all GP-CMCS/F127 hydrogels presented prominent pH-dependent swelling, owing to numerous hydroxyl and carboxyl groups of

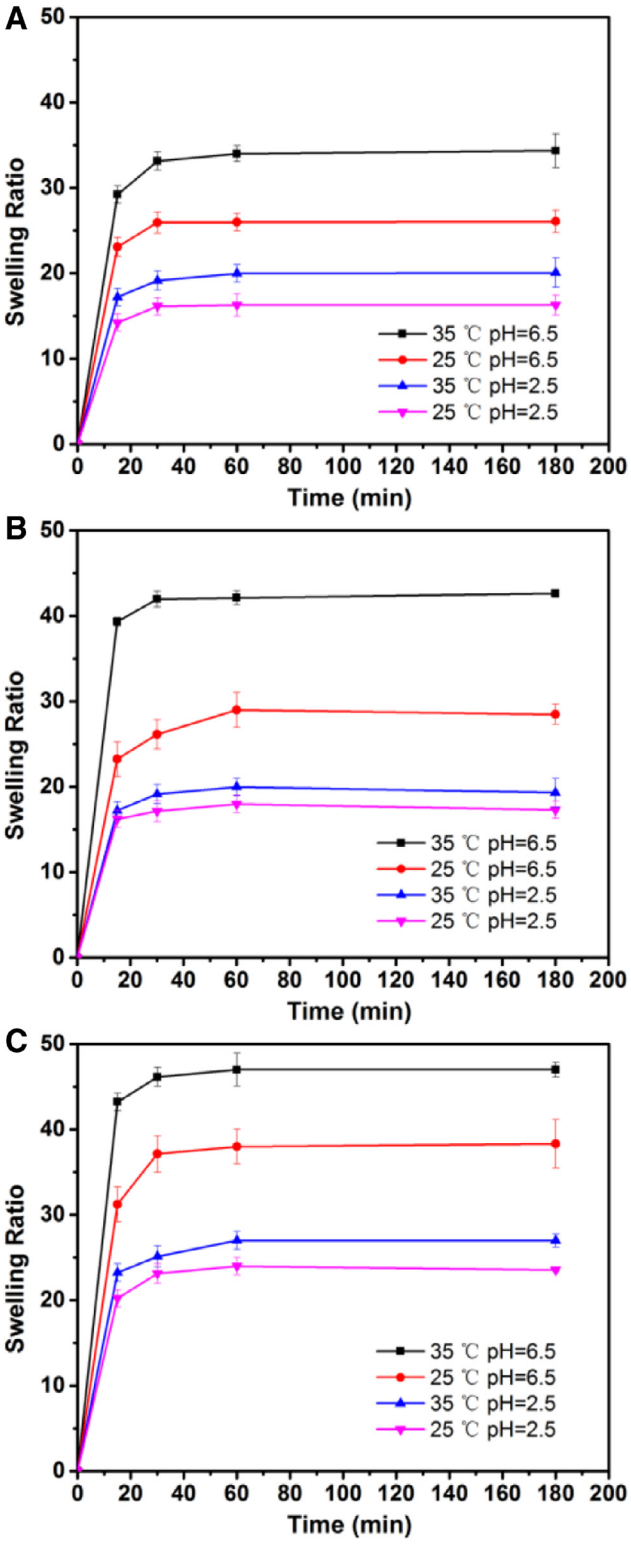

Fig. 9 – Swelling behaviors of GP-CMCS/F127 hydrogels with various CMCS-to-F127 weight ratios (A: 2.5/1.5; B: 3.0/1.0; C: 3.5/0.5) cross-linked by 0.4% (w/v) GP at four conditions (mean ± SD, $n = 3$).

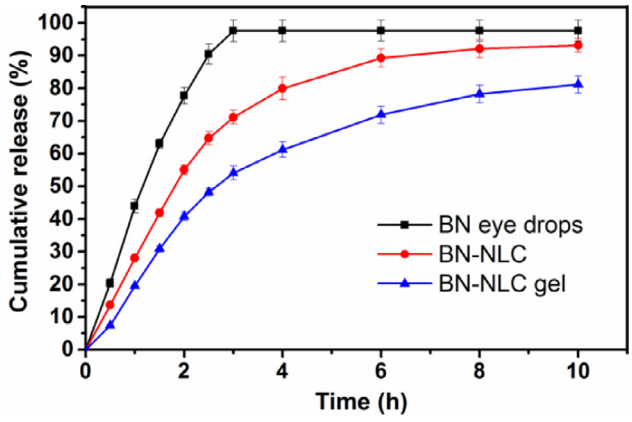

Fig. 10 – BN release profiles from various formulations at pH 6.5, 35 °C (mean ± SD, $n = 3$).

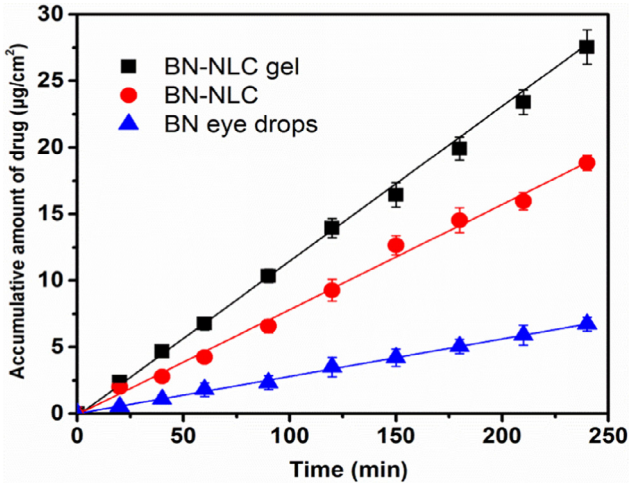

Fig. 11 – Transcorneal penetration profiles of various formulations (mean ± SD, $n = 3$).

CMCS [14]. At pH 2.5, SR values of GP-CMCS/F127 hydrogels were limited, because hydroxyl and carboxyl groups of CMCS in their neutral form (–OH and –COOH), which could form hydrogen bonds and absorb less water. On the contrary, SR values were higher at pH 6.5, owing to progressively ionized carboxyl groups of CMCS. The increase of charge density had a positive influence on the water uptake capacity by electrostatic repulsion force between the ionized groups, which resulted in an increase of swelling ratio of GP-CMCS/F127 hydrogel. In addition, temperature-dependent swelling is also observed in Fig. 9. F127 can self-assemble into micelles in aqueous solutions, with hydrophobic PPO blocks forming the core and relatively hydrophilic PEO blocks forming the shell. As the ambient temperature rise from 25 to 35 °C, the growing number and close packing of F127 micelles resulted in the decrease of SR [28]. Consequently, at pH 6.5, 35 °C, the swelling ratios of the hydrogels were much higher than those under other conditions, which demonstrated the dual pH- and thermosensitivity of the hydrogel. Interestingly, we can find from

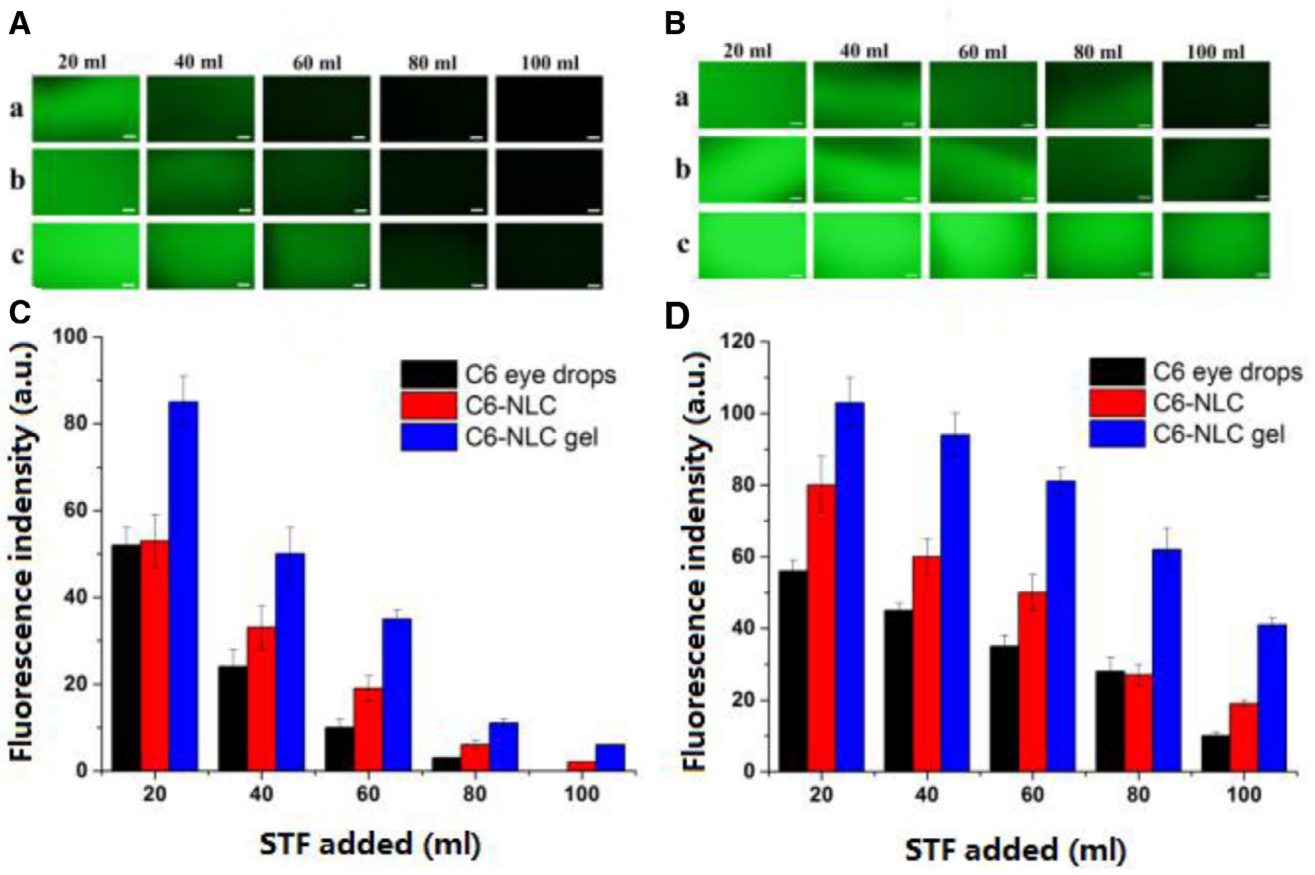

Fig. 12 – Retention of various C6 formulations on glass slides and excised corneas after several wash cycles using STF. Fluorescence microphotographs on (A) glass slides and (B) excised corneas: (a) C6 eye drops; (b) C6-NLC; (c) C6-NLC gel, Scale bar is 200 μm. Fluorescence indensity levels on (C) glass slides and (D) excised corneas (mean ± SD, $n = 3$).

Fig. 9 that SR values at 180 min markedly increased as the weight ratio of CMCS to F127 in the hydrogels rise at pH 6.5, 35 °C (34.35 of CMCS/F127-2.5/1.5; 42.64 of CMCS/F127-3.0/1.0; 47.01 of CMCS/F127-3.5/0.5), owing to the increase in the carboxylic group content. The highest SR values though the hydrogel with a CMCS-to-F127 weight ratio of 3.5:0.5 had, the thermo-sensitivity of it was not apparent, because of relatively low amount of F127. Accordingly, the hydrogel with a CMCS-to-F127 weight ratio of 3.0:1.0 was chosen for *in vitro* release study.

3.4. *In vitro release study*

In vitro release behaviors of baicalin are illustrated in Fig. 10. It is a biphasic drug release pattern that BN–NLC gel presented: a burst release appeared initially and afterwards a sustained release. The biphasic release pattern is beneficial to deliver ophthalmic anti-inflammatory drug, as it facilitates the rapid onset of drug initially and maintains a sustained release for a long time. Furthermore, the release rate of baicalin from BN–NLC gel was obviously slower than that from BN eye drops and BN–NLC. BN eye drops completed releasing within 3 h and the cumulative amount of baicalin released from BN–NLC was 89.27% after 6 h, while that from BN–NLC gel was 81.10% after 10 h. The results revealed that compared to BN eye drops and BN–NLC, BN–NLC gel would prolong the release of baicalin, owing to the three-dimensional network structure of the hydrogel as an additional diffusion barrier of the drug. In short, BN–NLC gel is a proper vehicle for the sustained release of baicalin.

Table 4 – Transcorneal penetration parameters of various preparations (mean ± SD, $n = 3$).

Sample	$P_{app} \times 10^5$ (cm/s)	$J_{ss} \times 10^4$ (μg/s/cm^2)	HL (%)
BN eye drops	1.30 ± 0.09	4.45 ± 0.53	84.62 ± 0.42
BN–NLC	4.13 ± 0.11	13.17 ± 0.64	79.09 ± 0.57
BN–NLC gel	5.80 ± 0.06	19.38 ± 0.41	78.16 ± 0.26

3.5. *Corneal permeation study*

Fig. 11 exhibits the corneal penetration profiles of BN eye drops, BN–NLC and BN–NLC gel, and the transcorneal penetration parameters of different formations are listed in Table 4. Straight lines were observed in Fig. 11, which demonstrated throughout the experimental conditions, the corneas were integrated with constant penetration rate [46]. The cornea is generally recognized as an effective barrier to drug delivery, including three main layers: outer lipophilic epithelium, middle hydrophilic stroma and inner lipophilic endothelium

[2,44]. As shown in Table 4, the P_{app} of BN–NLC was 3.18-fold *versus* BN eye drops, which could be ascribed to lipid matrixes. Lipid matrixes of NLC are biocompatible with corneal epithelia and could facilitate the transcorneal permeation of the entrapped drug [57]. In addition, the surfactants in BN–NLC could open the intercellular tight junctions among the corneal epithelia, improve the solubility of baicalin and enhance drug penetration. Moreover, BN–NLC gel can further increase the corneal penetration of baicalin, with 1.40-fold and 4.46-fold *versus* that of BN–NLC and BN eye drops, separately. The higher viscosity and moisture retention ability of hydrogels can increase residence time on ocular surface, prolong drug localization inside corneal tissues and act as a reservoir for BN delivery [2,58].

3.6. *Corneal hydration level study*

Hydration level (HL) is an index employed to investigate the extent of the corneal damage. As exhibited in Table 4, the HL of BN–NLC gel was 78.16 ± 0.26. The HL range of normal cornea is 76%–80% and a higher HL of 83%–92% indicates a damage to the epithelium and/or endothelium [58,59]. Accordingly, BN–NLC gel produced no significant corneal irritation and it is demonstrated to be promising for ophthalmic application.

3.7. *Precorneal retention study*

Precorneal retention study was carried out by a flow-through approach with fluorescence detection [50,60]. Fluorescence microphotographs and retention profiles of various formulations after washing with STF are presented in Fig. 12. Glass slides were used in non-mucosal control groups to investigate whether the mucoadhesion behavior could be simply due to the viscosity of the preparations, or especial mucoadhesive interactions. We can observe from Fig. 12A and C that C6 eye drops and C6-NLC washed off totally after 2 and 3 wash cycles, respectively. For C6-NLC gel, fluorescence signals can be detected after 5 wash cycles. The results of different formulations on the glass slide relied mainly on the viscosity of the preparations. Much higher viscosity of C6-NLC gel than C6 eye drops and C6-NLC led to stronger fluorescence signals after consecutive washes. As shown in Fig. 12B and D, compared to the glass slide groups, all formulations presented better retention on the surface of the cornea. However, significant decrease in fluorescence indensity of C6 eye drops and C6-NLC can be seen after 3 wash cycles. As expected, C6-NLC gel exhibited the strongest mucoadhesion, which could be ascribed to the penetration of C6 into the corneal epithelium with the help of surfactants. Moreover, with high viscosity and moisture retention ability, the NLC-based hydrogel can act as a precorneal drug reservoir and increase drug residence time on ocular surface.

4. Conclusions

In conclusion, we have successfully developed an innovative NLC-based hydrogel for ophthalmic drug delivery. The results have demonstrated that the hydrogel composed of CMCS and F127 crosslinked by GP is dual pH- and thermo-sensitive and the NLC-based hydrogel is an effective vehicle for drug delivery of baicalin. In conclusion, such a unique NLC-based hydrogel with dual pH- and thermo-sensitivity can combine the superiorities of macroscale drug delivery systems and nanomedicines, and will have a promising potential for application in ophthalmic drug delivery.

Conflicts of interest

The authors declare that there is no conflicts of interest.. The authors alone are responsible for the content and writing of this article.

Acknowledgments

The authors thank the National Natural Science Foundation of China (projects 81473163 and 81773670) for supporting the research.

Supplementary materials

Supplementary material associated with this article can be found, in the online version, at doi:10.1016/j.ajps.2018.08.002.

REFERENCES

[1] Gan L, Wang J, Jiang M, et al. Recent advances in topical ophthalmic drug delivery with lipid-based nanocarriers. Drug Discov Today 2013;18(5–6):290–7.
[2] Li J, Liu D, Tan G, Zhao Z, Yang X, Pan W. A comparative study on the efficiency of chitosan-N-acetylcysteine, chitosan oligosaccharides or carboxymethyl chitosan surface modified nanostructured lipid carrier for ophthalmic delivery of curcumin. Carbohydr Polym 2016;146:435–44.
[3] Zubairu Y, Negi LM, Iqbal Z, Talegaonkar S. Design and development of novel bioadhesive niosomal formulation for the transcorneal delivery of anti-infective agent: *in vitro* and *ex vivo* investigations. Asian J Pharm Sci 2015;10(4):322–30.
[4] Lin C, Metters AT. Hydrogels in controlled release formulations: Network design and mathematical modeling. Adv Drug Deliver Rev. 2006;58(12–13):1379–408.
[5] Bajpai AK, Shukla SK, Bhanu S, Kankane S. Responsive polymers in controlled drug delivery. Prog Polym Sci 2008;33(11):1088–118.
[6] Chen L, Tian Z, Du Y. Synthesis and pH sensitivity of carboxymethyl chitosan-based polyampholyte hydrogels for protein carrier matrices. Biomaterials 2004;25(17):3725–32.
[7] Qiu Y, Park K. Environment-sensitive hydrogels for drug delivery. Adv Drug Deliver Rev 2001;53(3):321–39.
[8] Wichterle O, Lim D. Hydrophilic gels for biological use. Nature 1960;185(4706):117–18.
[9] Gregorova A, Saha N, Kitano T, Saha P. Hydrothermal effect and mechanical stress properties of carboxymethylcellulose based hydrogel food packaging. Carbohydr Polym 2015;117:559–68.
[10] Drury JL, Mooney DJ. Hydrogels for tissue engineering: scaffold design variables and applications. Biomaterials 2003;24(24):4337–51.
[11] Heo DN, Castro NJ, Lee SJ, Noh H, Zhu W, Zhang LG. Enhanced bone tissue regeneration using a 3D printed

microstructure incorporated with a hybrid nano hydrogel. Nanoscale 2017;9(16):5055–62.
[12] Liu M, Song X, Wen Y, Zhu J, Li J. Injectable thermoresponsive hydrogel formed by alginate-g-poly(N-isopropylacrylamide) that releases doxorubicin-encapsulated micelles as a smart drug delivery system. ACS Appl Mater Inter 2017;9(41):35673–82.
[13] Chivukula P, Dušek K, Wang D, Dušková-Smrčková M, Kopečková P, Kopeček J. Synthesis and characterization of novel aromatic azo bond-containing pH-sensitive and hydrolytically cleavable IPN hydrogels. Biomaterials 2006;27(7):1140–51.
[14] Chen SC, Wu YC, Mi FL, Lin YH, Yu LC, Sung HW. A novel pH-sensitive hydrogel composed of N,O-carboxymethyl chitosan and alginate cross-linked by genipin for protein drug delivery. J Control Release 2004;96(2):285–300.
[15] Chung T, Liu D, Yang J. Effects of interpenetration of thermo-sensitive gels by crosslinking of chitosan on nasal delivery of insulin: *in vitro* characterization and *in vivo* study. Carbohydr Polym 2010;82(2):316–22.
[16] Wei Y, Xie R, Lin Y, et al. Structure formation in pH-sensitive hydrogels composed of sodium caseinate and N,O-carboxymethyl chitosan. Int J Biol Macromol 2016;89:353–9.
[17] Park KM, Bae JW, Joung YK, Shin JW, Park KD. Nanoaggregate of thermosensitive chitosan-Pluronic for sustained release of hydrophobic drug. Colloid Surf B 2008;63(1):1–6.
[18] Chen Y, Wu H, Sun J, Dong G, Wang T. Injectable and thermoresponsive self-assembled nanocomposite hydrogel for long-term anticancer drug delivery. Langmuir 2013;29(11):3721–9.
[19] Liu H, Yang Q, Zhang L, Zhuo R, Jiang X. Synthesis of carboxymethyl chitin in aqueous solution and its thermo- and pH-sensitive behaviors. Carbohydr Polym 2016;137:600–7.
[20] Kaihara S, Suzuki Y, Fujimoto K. In situ synthesis of polysaccharide nanoparticles via polyion complex of carboxymethyl cellulose and chitosan. Colloid Surf B 2011;85(2):343–8.
[21] Xing Z, Wang C, Yan J, Zhang L, Li L, Zha L. Dual stimuli responsive hollow nanogels with IPN structure for temperature controlling drug loading and pH triggering drug release. Soft Matter 2011;7(18):7992–7.
[22] Kamoun EA, Fahmy A, Taha TH, et al. Thermo-and pH-sensitive hydrogel membranes composed of poly(N-isopropylacrylamide)-hyaluronan for biomedical applications: influence of hyaluronan incorporation on the membrane properties. Int J Biol Macromol 2018;106:158–67.
[23] Al-Kinani AA, Zidan G, Elsaid N, Seyfoddin A, Alani AWG, Alany RG. Ophthalmic gels: past, present and future. Adv Drug Deliver Rev 2018;126:113–26.
[24] Agrawal AK, Das M, Jain S. In situ gel systems as 'smart' carriers for sustained ocular drug delivery. Expert Opin Drug Del 2012;9(4):383–402.
[25] Mohammed S, Chouhan G, Anuforom O, et al. Thermosensitive hydrogel as an *in situ* gelling antimicrobial ocular dressing. Mater Sci Eng C– Mater 2017;78:203–9.
[26] Elsherif M, Hassan MU, Yetisen AK, Butt H. Glucose sensing with phenylboronic acid functionalized hydrogel-based optical diffusers. ACS Nano 2018;12(3):2283–91.
[27] Niu G, Du F, Song L, et al. Synthesis and characterization of reactive poloxamer 407s for biomedical applications. J Controlled Release 2009;138(1):49–56.
[28] Baskan T, Tuncaboylu DC, Okay O. Tough interpenetrating Pluronic F127/polyacrylic acid hydrogels. Polymer 2013;54(12):2979–87.
[29] Lin C, Lin W, Yang M. Fabrication and characterization of ophthalmically compatible hydrogels composed of poly(dimethyl siloxane-urethane)/Pluronic F127. Colloid Surf B 2009;71(1):36–44.
[30] Yucel Falco C, Falkman P, Risbo J, Cárdenas M, Medronho B. Chitosan-dextran sulfate hydrogels as a potential carrier for probiotics. Carbohydr Polym 2017;172:175–83.
[31] De Clercq K, Schelfhout C, Bracke M, et al. Genipin-crosslinked gelatin microspheres as a strategy to prevent postsurgical peritoneal adhesions: *in vitro* and *in vivo* characterization. Biomaterials 2016;96:33–46.
[32] Liu Z, Zhou Q, Zhu J, et al. Using genipin-crosslinked acellular porcine corneal stroma for cosmetic corneal lens implants. Biomaterials 2012;33(30):7336–46.
[33] Butler MF, Ng YF, Pudney P. Mechanism and kinetics of the crosslinking reaction between biopolymers containing primary amine groups and genipin. J Polym Sci Pol Chem 2003;41(24):3941–53.
[34] Lai J. Biocompatibility of genipin and glutaraldehyde cross-linked chitosan materials in the anterior chamber of the eye. Int J Mol Sci 2012;13(9):10970–85.
[35] Yang L, Lan Y, Guo H, et al. Ophthalmic drug-loaded N,O-carboxymethyl chitosan hydrogels: synthesis, *in vitro* and *in vivo* evaluation. Acta Pharmacol Sin 2010;31(12):1625–34.
[36] Qin C, Fei J, Cui G, et al. Covalent-reaction-induced interfacial assembly to transform doxorubicin into nanophotomedicine with highly enhanced anticancer efficiency. Phys Chem Chem Phys 2017;19:23733–9.
[37] Gonzalez A, Tartara LI, Palma SD, Alvarez Igarzabal CI. Crosslinked soy protein films and their application as ophthalmic drug delivery system. Mater Sci Eng C – Mater 2015;51:73–9.
[38] Koo H, Lim K, Jung H, Park E. Anti-inflammatory evaluation of gardenia extract, geniposide and genipin. J Ethnopharmacol 2006;103(3):496–500.
[39] Shindo S, Hosokawa Y, Hosokawa I, Ozaki K, Matsuo T. Genipin inhibits IL-1β-induced CCL20 and IL-6 production from human periodontal ligament cells. Cell Physiol Biochem 2014;33(2):357–64.
[40] Jeon W, Hong H, Kim B. Genipin up-regulates heme oxygenase-1 via PI3-kinase-JNK1/2-Nrf2 signaling pathway to enhance the anti-inflammatory capacity in RAW264.7 macrophages. Arch Biochem Biophys 2011;512(2):119–25.
[41] Niamprem P, Srinivas SP, Tiyaboonchai W. Optimization of indomethacin loaded nanostructured lipid carriers. Asian J Pharm Sci 2016;11(1):174–5.
[42] Almeida H, Lobão P, Frigerio C, et al. Development of mucoadhesive and thermosensitive eyedrops to improve the ophthalmic bioavailability of ibuprofen. J Drug Deliv Sci Tec 2016;35:69–80.
[43] Gonzalez-Mira E, Nikolic S, Calpena AC, Antonia Egea M, Souto EB, Luisa Garcia M. Improved and safe transcorneal delivery of flurbiprofen by NLC and NLC-based hydrogels. J Pharm Sci 2012;101(2):707–25.
[44] Liu Z, Zhang X, Li J, Liu R, Shu L, Jin J. Effects of Labrasol on the corneal drug delivery of baicalin. Drug Deliver 2009;16(7):399–404.
[45] Liu Z, Zhang X, Wu H, et al. Preparation and evaluation of solid lipid nanoparticles of baicalin for ocular drug delivery system *in vitro* and *in vivo*. Drug Dev Ind Pharm 2010;37(4):475–81.
[46] Zhang W, Li X, Ye T, et al. Nanostructured lipid carrier surface modified with Eudragit RS 100 and its potential ophthalmic functions. Int J Nanomed 2014;9:4305–15.
[47] Huh HW, Zhao L, Kim SY. Biomineralized biomimetic organic/inorganic hybrid hydrogels based on hyaluronic acid and poloxamer. Carbohydr Polym 2015;126:130–40.
[48] Liu C, Lan Q, He W, et al. Octa-arginine modified lipid emulsions as a potential ocular delivery system for

disulfiram: a study of the corneal permeation, transcorneal mechanism and anti-cataract effect. Colloid Surf B 2017;160:305–14.
[49] Alvarado HL, Abrego G, Garduño-Ramirez ML, Clares B, Calpena AC, García ML. Design and optimization of oleanolic/ursolic acid-loaded nanoplatforms for ocular anti-inflammatory applications. Nanomed Nanotechnol 2015;11(3):521–30.
[50] Irmukhametova GS, Mun GA, Khutoryanskiy VV. Thiolated mucoadhesive and PEGylated nonmucoadhesive organosilica nanoparticles from 3-mercaptopropyltrimethoxysilane. Langmuir 2011;27(15):9551–6.
[51] Fathi M, Mozafari MR, Mohebbi M. Nanoencapsulation of food ingredients using lipid based delivery systems. Trends Food Sci Tech 2012;23(1):13–27.
[52] Li M, Gao L, Chen J, et al. Controllable release of interleukin-4 in double-layer sol-gel coatings on TiO_2 nanotubes for modulating macrophage polarization. Biomed Mater 2018;13(4):45008.
[53] Zhao J, Yan Y, Shang Y, et al. Thermosensitive elastin-derived polypeptide hydrogels crosslinked by genipin. Int J Polym Mater 2017;66(8):369–77.
[54] Wongkom L, Jimtaisong A. Novel biocomposite of carboxymethyl chitosan and pineapple peel carboxymethylcellulose as sunscreen carrier. Int J Biol Macromol 2017;95:873–80.
[55] Wang Y, Liu X, Zhang J, et al. Structural characterization and *in vitro* antitumor activity of polysaccharides from Zizyphus jujuba cv. Muzao RSC Adv 2015;5(11):7860–7.
[56] Costa-Júnior ES, Barbosa-Stancioli EF, Mansur AAP, Vasconcelos WL, Mansur HS. Preparation and characterization of chitosan/poly(vinyl alcohol) chemically crosslinked blends for biomedical applications. Carbohydr Polym 2009;76(3):472–81.
[57] Tan G, Yu S, Pan H, et al. Bioadhesive chitosan-loaded liposomes: a more efficient and higher permeable ocular delivery platform for timolol maleate. Int J Biol Macromol 2017;94:355–63.
[58] Schoenwald RD, Huang HS. Corneal penetration behavior of β-blocking agents I: physicochemical factors. J Pharm Sci 1983;72:1266–72.
[59] Moustafa MA, Elnaggar YSR, El-Refaie WM, Abdallah OY. Hyalugel-integrated liposomes as a novel ocular nanosized delivery system of fluconazole with promising prolonged effect. Int J Pharm 2017;534(1-2):14–24.
[60] Mun EA, Williams AC, Khutoryanskiy VV. Adhesion of thiolated silica nanoparticles to urinary bladder mucosa: effects of PEGylation, thiol content and particle size. Int J Pharm 2016;512(1):32–8.